Polymer 69 (2015) 17–24

Contents lists available at ScienceDirect

Polymer

journal homepage: www.elsevier.com/locate/polymer

High-pressure rheological analysis of CO_2-induced melting point depression and viscosity reduction of poly(ε-caprolactone)

S. Curia [a], D.S.A. De Focatiis [b], S.M. Howdle [a, *]

[a] University of Nottingham, School of Chemistry, University Park, Nottingham, NG72RD, UK
[b] University of Nottingham, Division of Materials, Mechanics and Structures, Faculty of Engineering, University Park, Nottingham, NG72RD, UK

ARTICLE INFO

Article history:
Received 27 February 2015
Received in revised form
13 May 2015
Accepted 14 May 2015
Available online 21 May 2015

Keywords:
Poly(ε-caprolactone)
Supercritical CO_2
Rheology

ABSTRACT

High-pressure rheology has been used to assess the effects of supercritical carbon dioxide ($scCO_2$) on the melting point (T_m) and viscosity of poly(ε-caprolactone) (PCL) over a range of temperatures and pressures up to 300 bar over a wide range of shear rates. Plots of the storage and loss moduli against temperature show a significant shift of T_m to lower temperatures in the presence of CO_2, indicating that the polymer crystals melt at temperatures much lower than the ambient pressure T_m.

Furthermore, a significant decrease in the viscosity of two PCL grades with different molecular weight (M_n ~ 10 kDa and 80 kDa) was also detected upon increasing the CO_2 pressure to 300 bar. Experimental viscosity data were fitted to the Carreau model to quantify the extent of the plasticising effects on the zero-shear viscosity and relaxation time under different conditions. Similar analyses were conducted under high-pressure nitrogen, to compare the effects obtained in the presence of a non-plasticising gas.

1. Introduction

In recent years there has been increasing interest in the use of high-pressure CO_2 as a reaction medium or plasticiser for polymer synthesis and processing [1–6]. CO_2 has been exploited as a solvent for polymerisations [7,8], as a foaming agent [1,9–13], for precipitation/separation [14], particle formation [15,16] and encapsulation [17].

High-pressure CO_2 is able to plasticise and effectively liquefy many polymers at temperatures below their glass transition temperatures (T_g) and melting points (T_m) [2,16,18–27], thereby opening up opportunities for new processes and incorporation of thermally labile molecules [17,28]. The CO_2-induced plasticisation mimics the effect of heating the polymer and it is characterised by an increased segmental and chain mobility [29]: the CO_2 molecules exhibit significant specific interactions with many polymers, mainly due to their large quadrupole moment [5,30]. These interactions often result in high sorption levels and decrease the intermolecular bonding between the chains [31]. This causes an increase in the free volume fraction (v_f) and therefore a higher mobility of the polymer chains, hence, leading to a decrease in viscosity with the CO_2 molecules acting as molecular lubricants [16,31].

Furthermore, the plasticisation is easily reversible: upon depressurisation, the supercritical solvent is removed and no residue is left. This use of CO_2 can be extremely valuable in the preparation of polymeric materials for food packaging and medical applications [16,29]. This, together with the accessible critical point of CO_2 (31.1 °C and 73.8 bar) and its non-flammability, non-toxicity and low price, make CO_2 a valuable renewable alternative to conventional solvents for polymer synthesis and processing.

PCL is a hydrophobic biodegradable polyester used in a wide range of applications such as food packaging, engineering materials and adhesives [32–36]. It is a semi-crystalline polyester with T_m ~ 55–70 °C and T_g ~ −60 °C that can be synthesised through ring-opening polymerisation of ε-caprolactone (ε-CL) using catalysts such as stannous octanoate or enzymes such as Candida Antarctica Lipase B [37,38].

The degradation of PCL occurs through the hydrolysis of its ester linkages under physiological conditions [37]. For this reason, PCL has also received much attention for use as an implantable, resorbable material and is already used in many medical applications such as drug delivery, sutures, dentistry and tissue engineering [9,12,37,39,40].

Nonetheless, molten PCL requires the use of high temperatures (above 140 °C) in order to achieve suitably low viscosities for

* Corresponding author. Tel.: +44 (0) 115 951 3486; fax: +44 (0) 115 846 8459.
E-mail address: Steve.Howdle@nottingham.ac.uk (S.M. Howdle).

http://dx.doi.org/10.1016/j.polymer.2015.05.026
0032-3861/

melt-processing [41]. These conditions are not acceptable for most medical applications where bioactive molecules are incorporated into the polymer, since these can be easily damaged by the high temperature. Lower temperature processing can be achieved by use of organic solvents, but this introduces unwelcome residues and can inactivate complex biomolecules [42]. In addition, the use of solvents imposes the need for an often challenging purification step for their removal after processing, thus making the overall process longer and more expensive.

The ability of CO_2 to be absorbed into PCL has been previously shown [43]. A change in the morphology of the polymer under CO_2 was also observed through infrared (IR) analysis by monitoring the carbonyl peak at 1720 cm^{-1} [44], and a decrease in the reptation time in the presence of high-pressure CO_2 was also found by the same group [45]. The plasticisation of this polymer under CO_2 was also studied optically [46,47] and through high-pressure calorimetry [48].

In addition, the diffusivity, solubility and specific volume of PCL/CO_2 solutions have been recently studied by coupling gravimetric and spectroscopic techniques [49,50]. Thus, there is no doubt that high-pressure studies for the development and optimisation of CO_2–assisted polymer processing techniques are topical and timely [3].

However, in the current literature there is a lack of any direct study of the loss and storage moduli as a function of temperature and pressure, and hence of the T_m of PCL in CO_2 through high-pressure rheological analysis. Therefore, we have investigated the use of high-pressure rheology to detect the melting point of PCL under CO_2 (1–120 bar) by conducting an oscillatory rheometric study under high-pressure conditions. Furthermore, only few shear viscosity data over a narrow shear rate range are available for PCL in the presence of $scCO_2$ [51]. Hence, the aims of this study are to measure the T_m depression of PCL through direct monitoring of the polymer viscoelasticity under CO_2, and to study the effects of compressed CO_2 and N_2 on the shear viscosities of two grades of PCL of different molar mass (10 kDa and 80 kDa) under various temperature and pressure conditions, over a wide range of shear rates. These data will contribute to the understanding of the structural state of semi-crystalline polyesters in the presence of $scCO_2$, and will aid the development of lower temperature melt processes of such polymers.

2. Materials and methods

2.1. Materials

PCL flakes (PCL10) with a density of 1.15 g/mL at 25 °C, M_n ~ 10 kDa and M_w ~ 14 kDa (by GPC) and PCL beads (PCL80) with a density of 1.15 g/mL at 25 °C, M_n ~ 80 kDa and M_w ~ 94 kDa (by GPC) were purchased from Sigma Aldrich (UK). The polymers were ground to obtain a powder before use. Supercritical Fluid Chromatography (SFC) grade 4.0 CO_2 (minimum purity 99.99%) and N_2 (99%) were purchased from BOC Special Gases (UK) and used as received.

2.2. Methods

2.2.1. T_m depression analysis

The effect of CO_2 on the T_m of PCL10 was studied using a Physica MCR301 rheometer (Anton Paar, Austria) equipped with Peltier temperature controller and a high-pressure cell (parallel plate geometry with 20 mm diameter and a 1 mm gap disc; PP20/Pr) with an upper operating pressure of 150 bar at room temperature and a maximum temperature of 300 °C. In a typical experiment 700 mg of polymer powder were added to the cup of the rheometer. A preliminary temperature ramp to 80 °C at 10 °C min^{-1}, followed by 5 min isothermal, was carried out to obtain a solid polymer disk upon cooling to 20 °C at 10 °C min^{-1}. Three preliminary strain amplitude sweeps at 1 Hz at ambient pressure were performed on the disk to identify a strain value within the linear viscoelastic region (LVR), and mean values are shown in Fig. 1. From these data, a strain amplitude of 1% was identified as suitable and well within the LVR.

The cell was then sealed and CO_2 was added using a syringe pump (Teledyne Isco 260D, USA). After pressurisation, the polymer was left to soak at 20 °C for 50 min to allow for CO_2 diffusion. A time study showed that longer times did not result in significant further drops in the T_m, see Supporting Information (SI) (Fig. S1–S4). The temperature of the cell was increased at a rate of 5 °C min^{-1} whilst imposing an oscillating strain of 1% to the sample at 1 Hz. Throughout the temperature scans the syringe remained connected to the cell to maintain the required pressure during heating. The shear storage modulus, G', and the loss modulus, G'', were recorded as a function of temperature. The T_m was taken as the temperature at which G'' is a maximum. All the experiments were repeated three times to give data confidence.

2.2.2. Shear viscosity high-pressure analyses

High-pressure rotational rheometric studies (continuous shearing with increasing shear rate) were carried out on PCL10 and PCL80 using an Anton Paar MCR 102 rheometer equipped a Teledyne Isco 260D syringe pump and with a 400 bar cell electrically heated (parallel plate geometry, PP20/Pr). The instrument was calibrated with mineral oils of standard viscosity supplied by Anton Paar.

The polymer powder was inserted in the cup and a preliminary temperature sequence was performed to melt the polymer. The sample was then allowed to equilibrate at 80 °C and the system sealed and pressurised. Samples were left for 50 min at pressure to soak. The rotational experiments were performed at constant temperature with logarithmically increasing the shear rate over a 2 min period from 10^{-3} to 10^{3} s^{-1} for PCL80, and from 1 to 10^{3} s^{-1} for PCL10. Due to the structural limits given by the ball-bearings in the pressure cell, the minimum torque that could be applied with our system was 200 μN m. When applying the minimum torque to two different liquids, the resulting minimum shear rate will be lower in the higher viscosity material. For this reason,

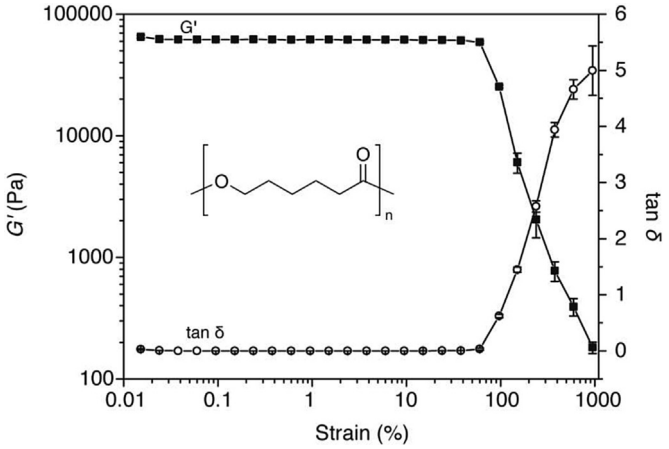

Fig. 1. Strain amplitude sweep showing the storage modulus, G', and loss tangent, tan δ, as a function of strain for PCL10 at ambient pressure and 20 °C at 1 Hz. The point at which the G' and tan δ start to deviate from the plateau values indicates departure from linear viscoelastic behaviour. For this reason, the oscillatory tests were conducted at 1 Hz with a strain amplitude of 1%. The polymer structure is shown (inset).

measurements carried out on low viscosity materials start at higher shear rates.

A matching set of experiments were carried out under N_2 at 60, 120 and 180 bar, by connecting a cylinder directly to the rheometer inlet through high-pressure Swagelok® tubing.

All rotational experiments were repeated at least three times; the mean values ±1 standard deviation are shown in the figures.

Temperature studies at ambient pressure and under CO_2 (at 120 bar) were conducted on PCL10 ($\dot{\gamma}$ = 12.0 s^{-1}) and PCL80 ($\dot{\gamma}$=0.1 s^{-1}) by increasing the temperature from 80 to 180 °C in 20 °C steps at 5 °C/min. After each ramp, a period of 10 min was imposed in order for sample to reach thermal equilibrium before the collection of 5 measurements, and then ramping to the next temperature.

Finally, transient shear experiment studies (time-dependent viscosity at constant applied shear rates, ranging from 0.25 s^{-1} to 5 s^{-1}) were conducted on PCL80 at ambient pressure (80 and 120 °C) and under CO_2 (80 °C, 120 bar) to investigate whether any phase separation and/or changes of solubility arise during shearing. Measurements of viscosity are plotted against time (Fig. S6 and S7). Due to the low viscosity and the equipment low torque limit, the same analysis could not be carried out on PCL10.

2.2.3. View cell plasticisation study

In order to observe visually the effect of CO_2 on the physical state of PCL10, a fixed volume view cell (100 mL) was used [52]. This view cell was manufactured in-house from 316-stainless steel with two thick sapphire windows located at the two ends of the cylindrical body which houses the inlet and outlet pipes.

In a typical experiment, 200 mg of sample were added in a glass vial and inserted in the view cell. The windows were sealed and clamped to the body, and CO_2 was added up to 50 bar. The temperature was raised to the desired value. When the temperature was stable, the CO_2 pressure was increased to the required value.

2.2.4. Differential Scanning Calorimetry (DSC)

DSC analyses on PCL10 were performed using a TA-Q2000 DSC (TA Instruments, USA) calibrated with sapphire and indium standards. In a standard experiment, the sample (6.00 ± 0.10 mg) was melted with a first heating scan up to 80 °C and cooled down to 20 °C (10 °C/min). A second heating scan, with the same temperature ramp settings of the oscillatory rheological analyses (80 °C; 5 °C/min), was then carried out. Between each ramp a 5-min isotherm was imposed.

The T_m was determined from the maximum of the endothermic peak and the degree of crystallinity (X_c) was calculated from Equation (1):

$$X_c = \frac{\Delta H_f(T_m)}{\Delta H_f^0\left(T_m^0\right)} \quad (1)$$

where $\Delta H_f(T_m)$ is the measured enthalpy of fusion and $\Delta H_f^0(T_m^0)$ is the enthalpy of fusion of a fully crystalline PCL, taken as 135.44 J/g [53–56].

The T_m as measured from DSC analysis is (64.6 ± 0.2) °C, whilst the X_c is (51.7 ± 0.5) %.

3. Results and discussion

3.1. Effect of pressure on T_m of PCL10

Typical oscillatory rheometric data obtained for PCL10 at ambient pressure show two distinct regions (Fig. 2): at lower temperatures G' has a value of ~60 kPa, typical of PCL above its T_g but below its T_m [57]. With increasing temperature there is a steep drop in the value of G' to ~2 kPa, as the material undergoes a thermal transition to a viscous fluid. There is an associated peak in G'' at the same temperature. This transition is associated with the melting of crystal spherulites in the polymer. The T_m at atmospheric pressure, as measured by rheology, is therefore 68.1 ± 0.6 °C, in good agreement with T_m reported elsewhere in the literature [37,45] and with that measured by DSC in this work (64.6 ± 0.2) °C.

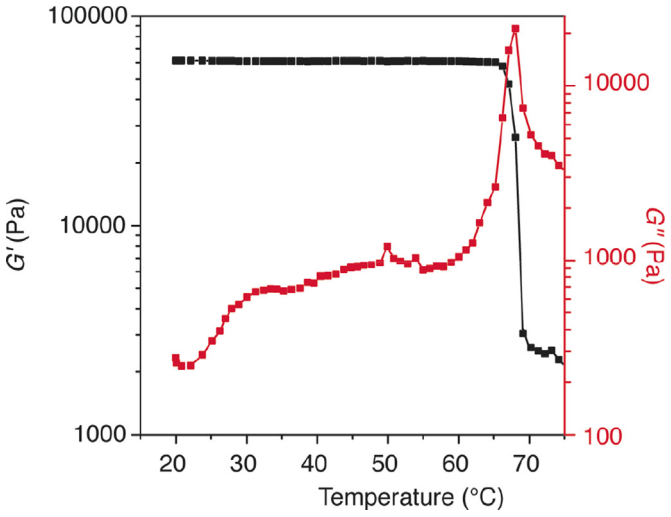

Fig. 2. Oscillatory rheometric measurements of G' and G'' as a function of temperature for PCL10 at ambient pressure. The dramatic changes in G' and G'' are produced by the melting of the polymer crystals. The average T_m obtained from the peak in G'' is 68.1 ± 0.6 °C.

The same experiment was performed over a range of pressures to evaluate the effect of high-pressure CO_2 on the T_m of PCL10. G' (Fig. 3) and G'' (Fig. 4) show a strong dependence upon temperature and CO_2 pressures. As expected, the shapes of the curves are similar to those obtained at ambient pressure. However, a comparison between the curves shows that the G' drop and G'' peak, and hence the T_m, are shifted to lower temperatures in the presence of pressurised CO_2.

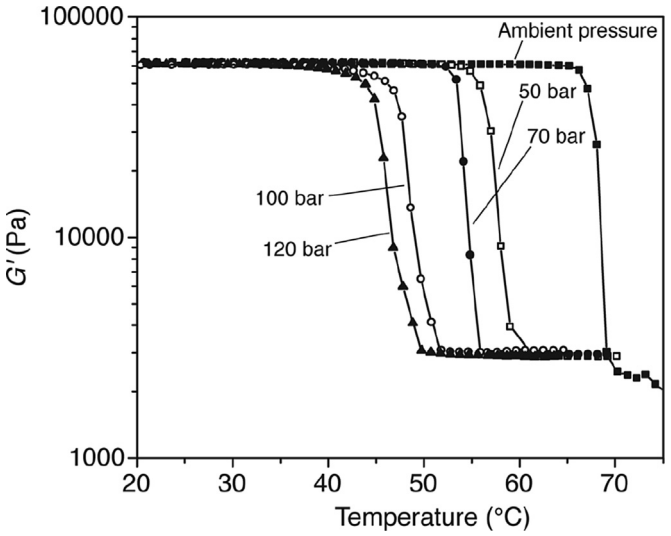

Fig. 3. Oscillatory rheometric measurements of G' as a function of temperature for PCL10 at a range of CO_2 pressures. The rapid decrease in G' is indicative of the polymer melting. Under high-pressure CO_2 the drop is shifted to lower temperatures, thus indicating a significant reduction in the T_m of the polymer (from 68.1 °C to 45.8 °C).

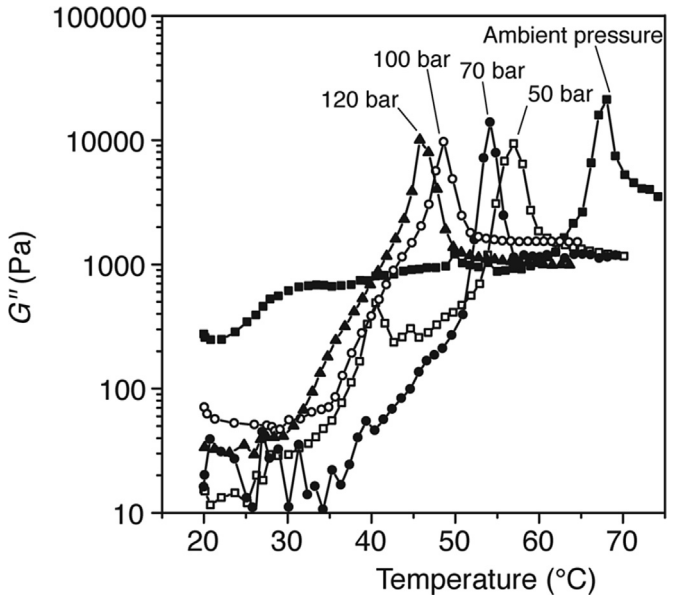

Fig. 4. Oscillatory rheometric measurements of G'' as a function of temperature for PCL10 at a range of CO_2 pressures. The peak in G'' is indicative of the polymer melting. Under CO_2 a significant reduction in the T_m of the polymer is observed.

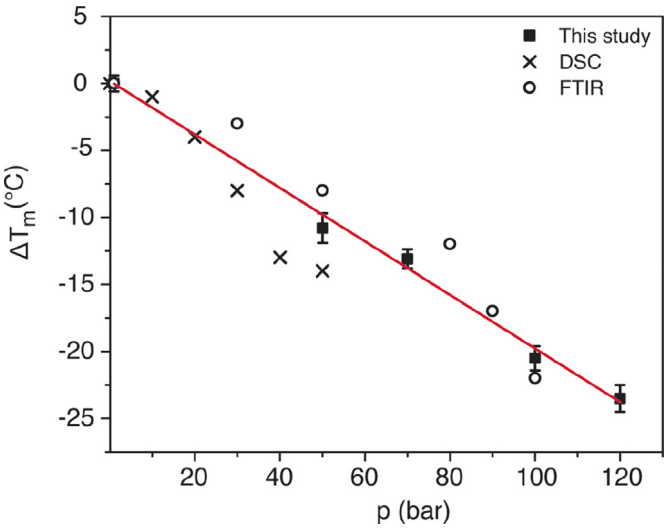

Fig. 5. Effect of CO_2 pressure on the change in T_m relative to atmospheric conditions, of PCL10 measured from the peak in G''. The results of this study follow a linear trend with high correlation ($R^2 > 0.99$). The data are in good agreement with the results obtained by other research groups through DSC [48] and FTIR [44].

This is a powerful demonstration of the ability of CO_2 to act as a temporary plasticiser for PCL, by diffusing into the polymer and interacting through Lewis acid/base interactions with the carbonyl groups of the backbone. As a result, the intermolecular interactions are weakened and the polymer can melt at temperatures much lower than the ambient pressure melting point.

The melting points measured from the peaks in G'' under high-pressure CO_2 have been plotted as a function of pressure and compared to two literature studies measuring the drop in T_m by DSC [48] and FTIR [44] (Fig. 5). The data show a high correlation ($R^2 > 0.99$) linear decrease with increasing pressure, moving from 68.1 °C at atmospheric conditions through to a significantly lower value of 45.8 °C under CO_2 at 120 bar.

Images from a view cell study clearly show that PCL10 initially appeared as a white powder (a), but in presence of CO_2 at 45 °C and 120 bar was gradually plasticised (Fig. 6). The view cell also confirmed the need for a long soaking time: after 15 min the sample was not fully plasticised (b), whilst after 50 min no solid residue could be observed (c). This rather long soaking time is most probably due to the high crystallinity of PCL10 (around 52% by DSC). It is indeed well known that CO_2 is able to diffuse and dissolve only in the amorphous regions of polymers [5,18,58], and that the T_m depression is given by both polymer-CO_2 interactions in the amorphous regions and crystallites characteristics (*e.g.* lamellar thickness and heat of fusion per unit of volume); hence, different effects will be expected for different levels of amorphous fractions [18,58].

Images from an additional view cell experiment carried out under high-pressure subcritical CO_2 can be found in the SI (Fig. S5).

3.2. Effect of pressure and molecular weight on the viscosity of PCL

Rotational rheometric experiments were performed at 80 °C on two PCL samples with different molecular weight, PCL10 and PCL80 (M_n ~ 10 kDa and ~80 kDa respectively) at a range of CO_2 pressures after 50 min soaking. The experiments were repeated under N_2, a non-plasticising gas, up to 180 bar, to gain a better understanding of plasticisation and compression effects. Data in the shear rate region between 10^{-3} and 10^{3} s^{-1} was obtained for PCL80. For PCL10, which is of lower molecular weight, and hence of lower viscosity, such low shear rates could not be investigated due to experimental limitations.

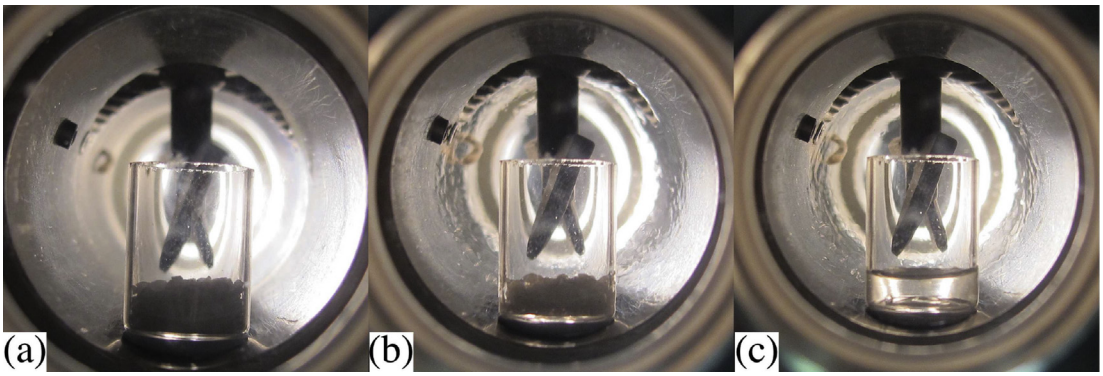

Fig. 6. Transitions observed for PCL10 in the view cell experiment: (a) initial polymer in the form of a white powder (room temperature and pressure); (b) sample not completely plasticised after 15 min (45 °C, 120 bar); (c) polymer fully plasticised after 50 min (45 °C, 120 bar). Although the mechanical stirrer is visible in the images, the sample was not stirred during the experiments.

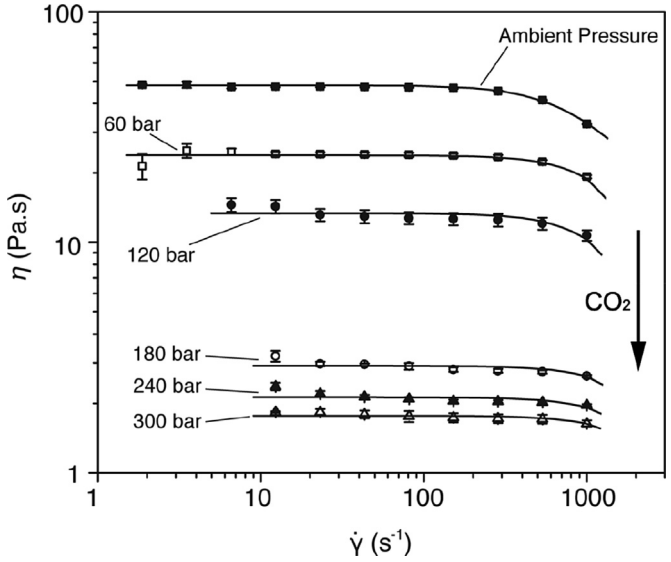

Fig. 7. Measurements of shear viscosity of PCL10 ($T = 80$ °C) at ambient pressure and under increasing CO_2 pressures. A significant reduction in the viscosity is observed with rising CO_2 pressure. The Carreau model (solid lines) is fitted to the data ($R^2 > 0.99$ for all the fits).

The measurements of viscosity as a function of shear rate at 80 °C at a range of CO_2 pressures for PCL10 exhibit Newtonian behaviour at low shear rates, followed by a shear-thinning region at shear rates above 300 s^{-1} (Fig. 7). The zero shear viscosity is dramatically decreased under CO_2, in agreement with results obtained on other polymers such as amorphous poly(lactic acid) [31], poly(ethylene glycol) [19], and poly(dimethylsiloxane) [59].

At pressures above 120 bar the shear thinning region was less detectable in this shear rate range. This is due to a decrease in the relaxation time of the polymer (higher chain mobility), which results in an extended Newtonian plateau [31]. The critical shear rate at which the shear thinning behaviour starts ($\dot{\gamma}_{cr}$) is, in fact, inversely proportional to the relaxation time [60–63].

The viscosity data were fitted to the Carreau model to enable quantitative determination of the relaxation time and of the zero shear viscosity. The model is given by:

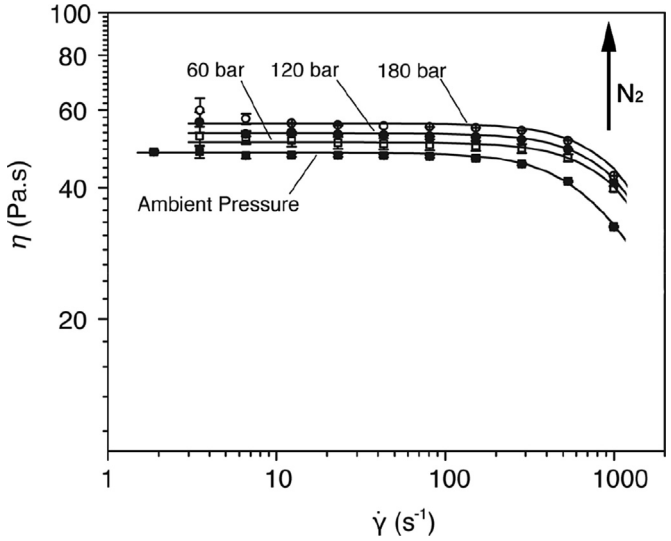

Fig. 8. Measurements of shear viscosity of PCL10 ($T = 80$ °C) at ambient pressure and under increasing N_2 pressures. A small increase in the viscosity is observed with increasing N_2 pressure. The Carreau model (solid lines) is fitted to the data ($R^2 > 0.99$ for all the sets of data).

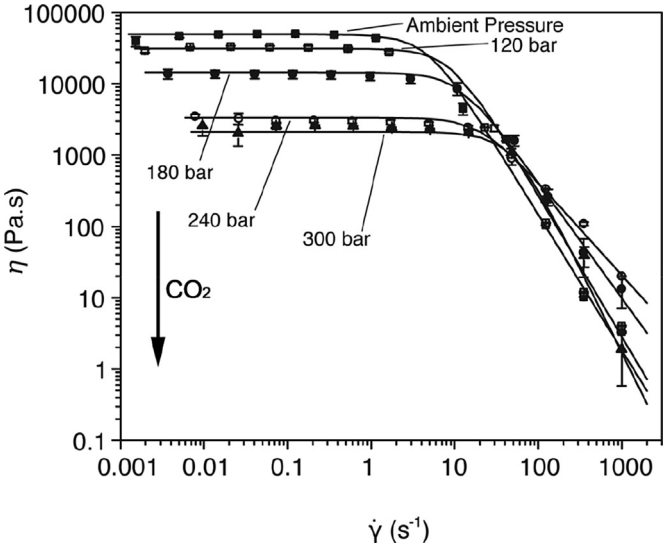

Fig. 9. Measurements of shear viscosity of PCL80 ($T = 80$ °C) at ambient pressure and under increasing CO_2 pressures. A significant reduction in the viscosity is observed with rising pressure. The Carreau model (solid lines) is fitted to the data ($R^2 > 0.99$ for all the fittings).

$$\eta(\dot{\gamma}) = \eta_0\left[1 + (\lambda\dot{\gamma})^2\right]^{-P} \tag{2}$$

where $\eta(\dot{\gamma})$ (Pa s) is the viscosity at a given shear rate $\dot{\gamma}$ (s^{-1}), η_0 (Pa s) is the zero shear viscosity, λ (s) is the relaxation time of the polymer and P is the Carreau exponent [31,64].

Measurements of viscosity as a function of shear rate at 80 °C at a range of N_2 pressures for PCL10 display a small but noticeable increase in viscosity with pressure (Fig. 8). Also, no significant changes in the extent of the zero shear plateau (hence, in $\dot{\gamma}_{cr}$) were observed, and shear thinning behaviour was always clearly observed within the shear rate range.

The ability of $scCO_2$ to plasticise higher MW PCL was confirmed by viscosity studies carried out on PCL80 (Fig. 9). The measurements of viscosity as a function of shear rate at 80 °C at a range of CO_2 pressures for PCL80 clearly show that this polymer has a much higher viscosity than PCL10, as expected from the higher degree of chain entanglement [60,65,66]. Also, $\dot{\gamma}_{cr}$ is considerably reduced. This is due to the longer relaxation time given by the increased chain length [60–63].

Nonetheless, a dramatic effect of the pressurised CO_2 on the viscosity was observed also for this higher MW polymer.

The zero shear viscosity is again significantly reduced with increasing CO_2 pressure, and the viscosity reduction is particularly significant in the shear rate region typical of polymer processing (between 1 and 4 s^{-1}) [62,67]. As expected, increasing CO_2 pressure results in higher $\dot{\gamma}_{cr}$ values and therefore in reduced relaxation times.

Table 1 shows a comparison of the viscosities of the two polymers at representative shear rates in the Newtonian plateau at ambient pressure, η_0^{amb}, and when plasticised by 300 bar CO_2,

Table 1
High-pressure CO_2-induced viscosity reduction of PCL10 and PCL80 in the Newtonian plateau at 80 °C.

M_n (kDa)	$\dot{\gamma}$ (s^{-1})	η_0^{amb} (Pa s)	$\eta_0^{300barCO_2}$ (Pa s)	η_0 reduction (%)
10	12.0	47.37 ± 0.40	1.84 ± 0.01	96.1
80	0.1	50,005.00 ± 429.19	2590.50 ± 280.79	94.8

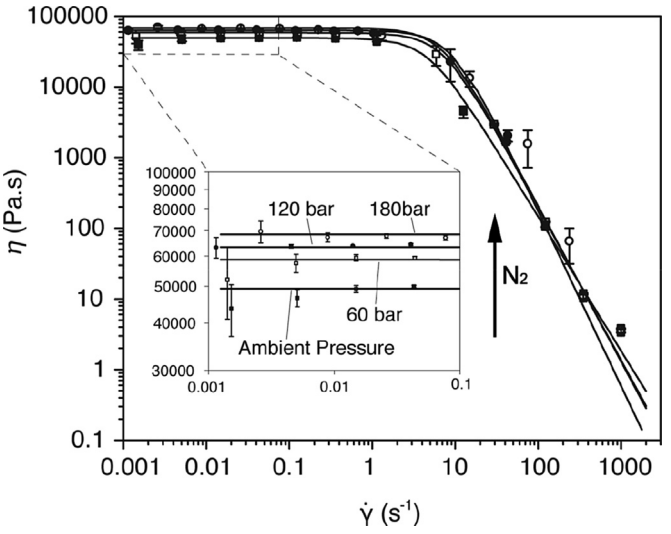

Fig. 10. Measurements of shear viscosity of PCL80 ($T = 80$ °C) at ambient pressure and under increasing N_2 pressures. A small increase in the zero shear viscosity is observed with rising pressure (zoomed in region). The Carreau model (solid lines) is fitted to the data ($R^2 > 0.99$ for all the fittings).

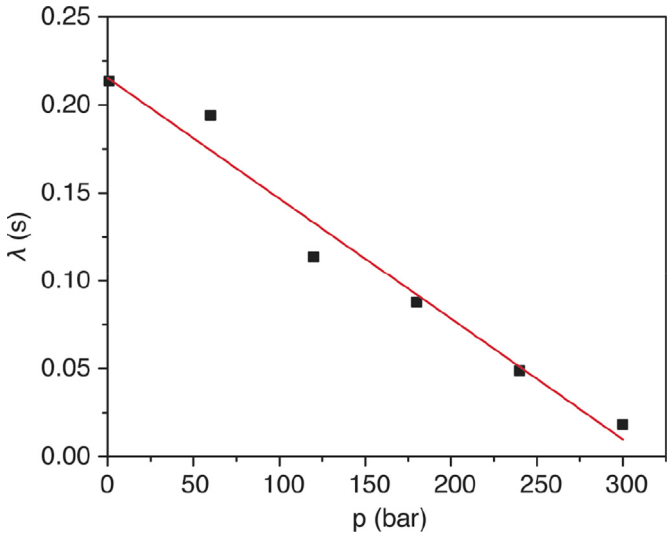

Fig. 12. Relaxation time as a function of CO_2 pressure obtained from Carreau model fits for PCL80 at $T = 80$ °C. A linear decrease ($R^2 > 0.96$) is observed.

$\eta_0^{300bar\ CO_2}$. Viscosities are reduced by around 95% for both polymers as a result of the plasticising effect.

Rotational rheological studies were carried out also for PCL80 in the presence of high-pressure N_2 (Fig. 10). Here again no viscosity decrease or changes in the extent of the Newtonian plateau could be observed. The zero shear viscosity increases with increasing pressure, although the effect is small.

The zero shear viscosities, calculated from the Carreau model fits for both polymers under CO_2 and N_2, have been plotted as a function of pressure (Fig. 11). A trend of increasing viscosity with pressure is found under N_2, and of decreasing viscosity with pressure under CO_2. Our data show that the pressure effects in the presence of N_2 give a viscosity increase in good agreement with the Barus equation

$$\eta_0(p) = \eta_0^{atm} e^{ap} \tag{3}$$

where $\eta_0(p)$ (Pa s) is the viscosity at pressure p (Pa), η_0^{atm} (Pa s) is the viscosity at atmospheric pressure and a (Pa^{-1}) is a pressure–viscosity coefficient [68]. The viscosity reduction with CO_2 pressure would require a negative pressure–viscosity coefficient in order fit the Barus equation, but the quality of fit would be vastly reduced as the reduction in log viscosity is not linear.

As stated before, the CO_2 plasticisation also results in a change in the relaxation time of the polymer, which is given by the higher chain mobility. In PCL80 a decrease in relaxation time with CO_2 pressure was recorded (Fig. 12). However, in PCL10 a decrease with a clear trend could not be observed. It is postulated that in the latter case the polymer chains are not sufficiently entangled because of their low MW, and therefore that the effect of plasticisation from the CO_2 may be less noticeable. A similar result has been observed with increasing temperature for poly(lactic acid) by Kelly *et al.* [31] who observed that at sufficiently high temperatures (well above T_g) no changes in relaxation time could be observed upon the addition of CO_2.

A final set of experiments were conducted at ambient pressure and under CO_2 (120 bar) over a temperature range of 80–180 °C in order to correlate the CO_2-induced viscosity depression to the temperature-induced reduction, and to obtain activation energies (E_a) with and without pressurised CO_2 (Table 2).

The zero shear viscosities of PCL10 ($\dot{\gamma} = 12.0\ s^{-1}$) and PCL80 ($\dot{\gamma}$=0.1 s^{-1}) are shown as a function of temperature in an Arrhenius plot (Fig. 13).

As expected, the fittings show that the E_a of the polymer is reduced under CO_2 (Table 2). Furthermore, the data show the

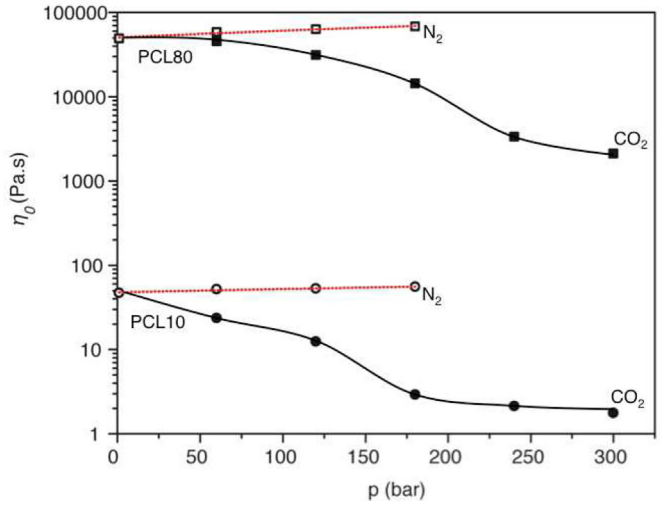

Fig. 11. Zero shear viscosity of PCL10 and PCL80 (T = 80 °C) under CO_2 and N_2. A small increase in the zero shear viscosity is observed on raising the N_2 pressure (empty symbols), whilst a decrease is seen under CO_2 (black symbols). The data collected under N_2 were fitted to the Barus equation (red dotted lines) with high correlation ($R^2 > 0.99$ for all the fittings). The black solid lines connecting the CO_2 data have been drawn as a guide to the eye. (For interpretation of the references to colour in this figure legend, the reader is referred to the web version of this article.)

Table 2
E_a reduction for PCL under CO_2.

MW (kDa)	E_a (kJ/mol)		Reduction (%)
	Ambient	120 bar	
80	29.59 ± 0.20	26.96 ± 0.18	8.9
10	31.27 ± 0.67	27.50 ± 0.35	12.1

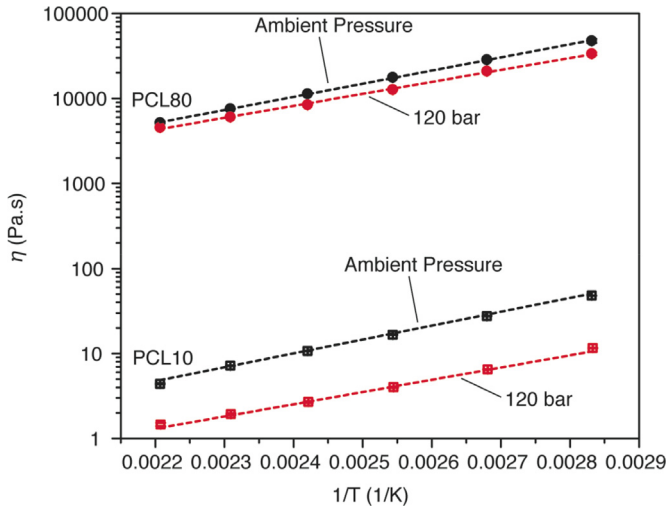

Fig. 13. Arrhenius plot of zero shear viscosity as a function of temperature for PCL10 and PCL80 at ambient pressure and under CO_2 (120 bar). In PCL10, a 91% reduction in the viscosity is obtained between 80 °C and 180 °C, whilst an 88% reduction is observed for PCL80 in the same temperature range. The data were fitted to an Arrhenius equation ($R^2 > 0.99$).

dramatic effect of processing with CO_2. For example, for PCL10, processing at 240 bar of CO_2 at 80 °C results in a viscosity (~3 Pa s) which is equivalent to processing at 180 °C at ambient pressure conditions. For PCL80, exposure to 240 bar of CO_2 at 80 °C produces a viscosity (~3 kPa s) which is even lower than the ambient pressure viscosity obtained at 180 °C (~6 kPa s). Therefore, these measurements demonstrate the significant opportunities that high-pressure CO_2 processing of polymers could deliver in terms of energy saving and processing of thermally labile materials [17].

4. Conclusions

High-pressure rheology was employed to demonstrate clearly the ability of CO_2 to plasticise PCL at supercritical and even subcritical (60 bar) conditions at 80 °C. For the first time, interpretation of the viscoelastic moduli with temperature plots have been used to show that by adding CO_2 it is possible to lower the melting point of PCL by more than 20 °C (from 68.1 to 45.8 °C). This provides a rheological viewpoint to the CO_2-induced T_m depression of this polymer that correlates well with previous studies using DSC and IR spectroscopy, and a linear drop in T_m with increasing CO_2 pressure was observed.

The viscosity of PCLs of different molecular weights decreased significantly when pressurised CO_2 was added. The reductions observed at 80 °C and 180 bar are comparable to those achieved at 180 °C at ambient pressure. At 300 bar 96% decrease in viscosity relative to ambient pressure was achieved for the 10 kDa polymer, whilst a 95% reduction was obtained for the 80 kDa polymer.

The Carreau model was employed for determination of the zero shear viscosity and the relaxation time, both of which decreased with increasing CO_2 pressure. By contrast, the effect of a non-plasticising gas, N_2, was to increase the zero shear viscosity.

In this paper we demonstrated the use of a high-pressure rheometer to detect the T_m depression of polymers under CO_2, highlighting the ability of CO_2 to act as a green and efficient temporary plasticiser that allows for processing of degradable polymers at significantly lower temperatures (80 °C rather than 180 °C).

Acknowledgements

We thank Richard Wilson, Pete Fields and Mark Guyler (University of Nottingham) for the technical input with the high-pressure equipment.

The research leading to these results has received funding from the People Programme (Marie Curie Actions) of the European Union's Seventh Framework Programme FP7/2007-2013/under REA grants agreement No. [289253].

Abbreviations

CL	caprolactone
DSC	differential scanning calorimetry
E_a	activation energy for viscous flow
IR	infrared
MW	molecular weight
PCL	poly(ε-caprolactone)
$scCO_2$	supercritical carbon dioxide
SI	supporting information
T_g	glass transition temperature
T_m	melting point
X_c	degree of crystallinity

Appendix A. Supplementary data

Supplementary data related to this article can be found at http://dx.doi.org/10.1016/j.polymer.2015.05.026.

References

[1] Tsioptsias C, Paraskevopoulos MK, Christofilos D, Andrieux P, Panayiotou C. Polymeric hydrogels and supercritical fluids: the mechanism of hydrogel foaming. Polymer 2011;52:2819–26.
[2] Gutiérrez C, Garcia MT, Curia S, Howdle SM, Rodriguez JF. The effect of CO_2 on the viscosity of polystyrene/limonene solutions. J Supercrit Fluids 2014;88:26–37.
[3] Picchioni F. Supercritical carbon dioxide and polymers: an interplay of science and technology. Polym Int 2014;63(8):1394–9.
[4] Jennings J, Beija M, Kennon JT, Willcock H, O'Reilly RK, Rimmer S, et al. Advantages of block copolymer synthesis by RAFT-controlled dispersion polymerization in supercritical carbon dioxide. Macromolecules 2013;46:6843–51.
[5] Davies OR, Lewis AL, Whitaker MJ, Tai H, Shakesheff KM, Howdle SM. Applications of supercritical CO_2 in the fabrication of polymer systems for drug delivery and tissue engineering. Adv Drug Deliv Rev 2008;60:373–87.
[6] Yang F, Manitiu M, Kriegel R, Kannan RM. Structure, permeability, and rheology of supercritical CO_2 dispersed polystyrene-clay nanocomposites. Polymer 2014;55:3915–24.
[7] Du L, Kelly JY, Roberts GW, DeSimone JM. Fluoropolymer synthesis in supercritical carbon dioxide. J Supercrit Fluids 2009;47:447–57.
[8] Jennings J, Beija M, Richez AP, Cooper SD, Mignot PE, Thurecht KJ, et al. One-pot synthesis of block copolymers in supercritical carbon dioxide: a simple versatile route to nanostructured microparticles. J Am Chem Soc 2012;134:4772–81.
[9] Tsivintzelis I, Pavlidou E, Panayiotou C. Biodegradable polymer foams prepared with supercritical CO_2–ethanol mixtures as blowing agents. J Supercrit Fluids 2007;42:265–72.
[10] Monnereau L, Urbanczyk L, Thomassin J-M, Pardoen T, Bailly C, Huynen I, et al. Gradient foaming of polycarbonate/carbon nanotube based nanocomposites with supercritical carbon dioxide and their EMI shielding performances. Polymer 2015;59:117–23.
[11] Monnereau L, Urbanczyk L, Thomassin J-M, Alexandre M, Jérôme C, Huynen I, et al. Supercritical CO_2 and polycarbonate based nanocomposites: a critical issue for foaming. Polymer 2014;55:2422–31.
[12] Jenkins MJ, Harrison KL, Silva MMCG, Whitaker MJ, Shakesheff KM, Howdle SM. Characterisation of microcellular foams produced from semi-crystalline PCL using supercritical carbon dioxide. Eur Polym J 2006;42:3145–51.
[13] Gualandi C, White LJ, Chen L, Gross RA, Shakesheff KM, Howdle SM, et al. Scaffold for tissue engineering fabricated by non-isothermal supercritical carbon dioxide foaming of a highly crystalline polyester. Acta Biomater 2010;6:130–6.

[14] Bungert B, Sadowski G, Arlt W. Supercritical antisolvent fractionation: measurements in the systems monodisperse and bidisperse polystyrenecyclohexanecarbon dioxide. Fluid Phase Equilibria 1997;139:349–59.
[15] Nalawade SP, Picchioni F, Janssen LPBM. Batch production of micron size particles from poly(ethylene glycol) using supercritical CO_2 as a processing solvent. Chem Eng Sci 2007;62:1712–20.
[16] Kelly CA, Naylor A, Illum L, Shakesheff KM, Howdle SM. Supercritical CO2: a clean and low temperature approach to blending PDLLA and PEG. Adv Funct Mater 2012;22:1684–91.
[17] Howdle SM, Watson MS, Whitaker MJ, Davies MC, Shakesheff KM, Popov VK, et al. Supercritical fluid mixing: preparation of thermally sensitive polymer composites containing bioactive materials. Chem Commun 2001:109–10.
[18] Zhang Z, Handa YP. CO_2-assisted melting of semicrystalline polymers. Macromolecules 1997;30:8505–7.
[19] Gourgouillon D, Avelino HMNT, Fareleira JMNA, Nunes da Ponte M. Simultaneous viscosity and density measurement of supercritical CO_2-saturated PEG 400. J Supercrit Fluids 1998;13:177–85.
[20] Alessi P, Cortesi A, Kikic I, Vecchione F. Plasticization of polymers with supercritical carbon dioxide: experimental determination of glass-transition temperatures. J Appl Polym Sci 2002;88:2189–93.
[21] Boyer SAE, Grolier JPE. Modification of the glass transitions of polymers by high-pressure gas solubility. Pure Appl Chem 2005;77:593–603.
[22] Lee M, Tzoganakis C, Park CB. Extrusion of PE/PS blends with supercritical carbon dioxide. Polym Eng Sci 1998;38:1112–20.
[23] Zhang Z, Handa YP. An in-situ study of plasticization of polymers by high-pressure gases. J Polym Sci Part B Polym Phys 1998;36:977–83.
[24] J.M.D.S, Royer Joseph R, Khan Saad A. High-pressure rheology and viscoelastic scaling predictions of polymer melts containing liquid and supercritical carbon dioxide. J Polym Sci Part B Polym Phys 2001;39:3055–66.
[25] Pini R, Storti G, Mazzotti M, Tai H, Shakesheff KM, Howdle SM. Sorption and swelling of poly(DL-lactic acid) and poly(lactic-co-glycolic acid) in supercritical CO_2: an experimental and modeling study. J Polym Sci Part B Polym Phys 2008;46:483–96.
[26] Yu L, Liu H, Chen L. Thermal behaviors of polystyrene plasticized with compressed carbon dioxide in a sealed system. Polym Eng Sci 2009;49:1800–5.
[27] Iguchi M, Hiraga Y, Kasuya K, Aida TM, Watanabe M, Sato Y, et al. Viscosity and density of poly(ethylene glycol) and its solution with carbon dioxide at 353.2K and 373.2K at pressures up to 15MPa. J Supercrit Fluids 2015;97:63–73.
[28] Ginty PJ, Barry JJA, White LJ, Howdle SM, Shakesheff KM. Controlling protein release from scaffolds using polymer blends and composites. Eur J Pharm Biopharm 2008;68:82–9.
[29] Kazarian SG. Polymer processing with supercritical fluids. Polym Sci Ser C 2000;42:78–101.
[30] Cooper AI. Polymer synthesis and processing using supercritical carbon dioxide. J Mater Chem 2000;10:207–34.
[31] Kelly CA, Howdle SM, Shakesheff KM, Jenkins MJ, Leeke GA. Viscosity studies of poly(DL-lactic acid) in supercritical CO2. J Polym Sci Part B Polym Phys 2012;50:1383–93.
[32] Koenig MF, Huang SJ. Biodegradable blends and composites of polycaprolactone and starch derivatives. Polymer 1995;36:1877–82.
[33] Mecham S, Sentman A, Sambasivam M. Amphiphilic silicone copolymers for pressure sensitive adhesive applications. J Appl Polym Sci 2010;116:3265–70.
[34] Ebnesajjad S. Plastic films in food packaging: materials, technology and applications. Elsevier Science; 2012.
[35] Alix S, Mahieu A, Terrie C, Soulestin J, Gerault E, Feuilloley MGJ, et al. Active pseudo-multilayered films from polycaprolactone and starch based matrix for food-packaging applications. Eur Polym J 2013;49:1234–42.
[36] Munoz-Bonilla A, Cerrada ML, Fernandez-Garcia M, Kubacka A, Ferrer M, Fernandez-Garcia M. Biodegradable polycaprolactone-titania nanocomposites: preparation, characterization and antimicrobial properties. Int J Mol Sci 2013;14:9249–66.
[37] Woodruff MA, Hutmacher DW. The return of a forgotten polymer—Polycaprolactone in the 21st century. Prog Polym Sci 2010;35:1217–56.
[38] Loeker FC, Duxbury CJ, Kumar R, Gao W, Gross RA, Howdle SM. Enzyme-catalyzed ring-opening polymerization of epsilon-caprolactone in supercritical carbon dioxide. Macromolecules 2004;37:2450–3.
[39] Xu Q, Ren X, Chang Y, Wang J, Yu L, Dean K. Generation of microcellular biodegradable polycaprolactone foams in supercritical carbon dioxide. J Appl Polym Sci 2004;94:593–7.
[40] Fanovich MA, Jaeger P. Sorption and diffusion of compressed carbon dioxide in polycaprolactone for the development of porous scaffolds. Mater Sci Eng C 2012;32:961–8.
[41] Kapoor B, Bhattacharya M. Transient shear and extensional properties of biodegradable polycaprolactone. Polym Eng Sci 1999;39:676–87.
[42] Fu K, Klibanov AM, Langer R. Protein stability in controlled-release systems. Nat Biotechnol 2000;18:24–5.
[43] Gary Leeke JC, Jenkins Mike. Solubility of supercritical carbon dioxide in polycaprolactone (CAPA 6800) at 313 and 333 K. J Chem Eng Data 2006;51:1877–9.
[44] Kelly CA, Harrison KL, Leeke GA, Jenkins MJ. Detection of melting point depression and crystallization of polycaprolactone (PCL) in scCO_2 by infrared spectroscopy. Polym J 2013;45:188–92.
[45] Kelly CA, Murphy SH, Leeke GA, Howdle SM, Shakesheff KM, Jenkins MJ. Rheological studies of polycaprolactone in supercritical CO_2. Eur Polym J 2013;49:464–70.
[46] Lian Z, Epstein SA, Blenk CW, Shine AD. Carbon dioxide-induced melting point depression of biodegradable semicrystalline polymers. J Supercrit Fluids 2006;39:107–17.
[47] Lian Z, Shine AD. Thermodynamic and fluid dynamic study of the Polymer Liquefaction by Using Supercritical Solvation (PLUSS) Process. Polym Mater Sci Eng 2005;93:890–1.
[48] Murphy S. Melting point depression in biodegradable polyesters, in: school of engineering. Department of Metallurgy and Materials, University of Birmingham; 2011. p. 100.
[49] Pastore Carbone MG, Di Maio E, Scherillo G, Mensitieri G, Iannace S. Solubility, mutual diffusivity, specific volume and interfacial tension of molten PCL/CO_2 solutions by a fully experimental procedure: effect of pressure and temperature. J Supercrit Fluids 2012;67:131–8.
[50] Pastore Carbone MG, Di Maio E, Musto P, Braeuer A, Mensitieri G. On the unexpected non-monotonic profile of specific volume observed in PCL/CO_2 solutions. Polymer 2015;56:252–5.
[51] Di Maio E, Iannace S, Mensitieri G, Nicolais L. A predictive approach based on the Simha–Somcynsky free-volume theory for the effect of dissolved gas on viscosity and glass transition temperature of polymeric mixtures. J Polym Sci Part B Polym Phys 2006;44:1863–73.
[52] Licence P, Dellar MP, Wilson RGM, Fields PA, Litchfield D, Woods HM, et al. Large-aperture variable-volume view cell for the determination of phase-equilibria in high pressure systems and supercritical fluids. Rev Sci Instrum 2004;75:3233–6.
[53] Crescenzi V, Manzini G, Calzolari G, Borri C. Thermodynamics of fusion of poly-β-propiolactone and poly-ε-caprolactone. comparative analysis of the melting of aliphatic polylactone and polyester chains. Eur Polym J 1972;8:449–63.
[54] Khambatta FB, Warner F, Russell T, Stein RS. Small-angle x-ray and light scattering studies of the morphology of blends of poly(ε-caprolactone) with poly(vinyl chloride). J Polym Sci Polym Phys Ed 1976;14:1391–424.
[55] Wang J, Cheung MK, Mi Y. Miscibility and morphology in crystalline:amorphous blends of polycaprolactone):poly4-vinylphenol) as studied by DSC, FTIR, and 13C solid state NMR. Polymer 2002;43:1357–64.
[56] Ikeda H, Ohguma Y, Nojima S. Composition dependence of crystallization behavior observed in crystalline-crystalline diblock copolymers. Polym J 2008;40:241–8.
[57] Menard KP. Dynamic mechanical analysis : a practical introduction/Kevin P. Menard. CRC Press; 2008.
[58] Handa YP, Zhiyi Z, Betty W. Effect of compressed CO_2 on phase transitions and polymorphism in syndiotactic polystyrene. Macromolecules 1997;30:8499–504.
[59] Gerhardt LJ, Garg A, Manke CW, Gulari E. Concentration-dependent viscoelastic scaling models for polydimethysiloxane melts with dissolved carbon dioxide. J Polym Sci Part B Polym Phys 1998;36:1911–8.
[60] Bird RB, Armstrong RC, Hassager O. Dynamics of polymeric liquids. 2nd ed., vol. 1. Fluid Mechanics; 1987.
[61] Swallowe GM. In: Swallowe GM, editor. Mechanical properties and testing of polymers: an A–Z reference. Kluwer Academic; 1999.
[62] Chung CI. Extrusion of polymers: theory and practice. Hanser Gardner Publications; 2000.
[63] Anderson BJ. U.o.I.a. Urbana-Champaign, rheology and microstructure of filled polymer melts. University of Illinois at Urbana-Champaign; 2008.
[64] Carreau PJ. Rheological equations from molecular network theories. Trans Soc Rheol 1972;16:99–127.
[65] Colby RH, Fetters LJ, Graessley WW. The melt viscosity-molecular weight relationship for linear polymers. Macromolecules 1987;20:2226–37.
[66] Cooper-White JJ, Mackay ME. Rheological properties of poly(lactides). Effect of molecular weight and temperature on the viscoelasticity of poly(l-lactic acid). J Polym Sci Part B Polym Phys 1999;37:1803–14.
[67] Osswald TA. Polymer processing fundamentals. Hanser; 1998.
[68] Barus C. Note on the dependence of viscosity on pressure and temperature. Proc Am Acad Arts Sci 1891;27:13–8.